Оптический журнал

Физическая оптика

DOI:10.17586/1023-5086-2018-85-06-06-11

Single reflection nanocavity enhanced transmission efficiency of nanoplasmonic wavelength demultiplexer

© 2018 Qi Ma*, **; Guangqiang Liu**; Yiqing Chen*; Qian Zhao**; Shaosong Yang**; Jing Guo**; Weiping Cai**

*School of Materials Science and Engineering, Hefei University of Technology, Hefei, Anhui 230009, P. R. China.
**Key Lab of Materials Physics, Anhui Key Lab of Nanomaterials and Nanotechnology, Institute of Solid State Physics, Chinese Academy of Sciences, Hefei 230031, P.R. China

E-mail: liugq@issp.ac.cn, chenyq63@126.com

Submitted 11.12.2017

As a kind of nanostructure device, Surface Plasmon Polaritons (SPPs) nanostructure filter can realize the effective manipulation of photons at nanometer or subwavelength scale. Among them, kinds of resonator-based multiplexer channel drop filters have been proposed and studied widely. However, a main problem is that the transmission efficiencies of such filters are relatively low. Thus, reflection cavities are designed for enhancing the transmission efficiency obviously. However, traditional demultiplexer usually requires several reflection cavities, because only one mode is utilized in a reflection cavity. In this paper, single reflection cavity is firstly designed to enhance the transmission efficiency of three channels at the same time via utilizing multiple modes in the reflection cavity. The theory and simulation analysis confirm the validity of such structure, the transmission efficiency of the three channels can be doubled. We believe this work provides novel notions for the design for demultiplexer filter.

Keywords: *surface plasmons, wavelength filtering, multiplexing, subwave length.*

OCIS codes: *240.6680, 130.7408, 060.4230, 030.4070.*

Повышение эффективности пропускания каналов наноплазмонного волноводного демультиплексора с использованием единичного отражательного нанорезонатора

© 2018 г. Qilin Ma; Guangqiang Liu; Yiqing Chen; Qian Zhao; Shaosong Yang; Jing Guo; Weiping Cai

Наноструктурный фильтр на основе поверхностных плазмон-поляритонов (Surface Plasmon Polaritons, SPP) позволяет обеспечить эффективные воздействия на фотоны, манипулируя на нанометровом или субмикронном уровне масштаба устройств. Предложенные и широко исследованные ранее разновидности фильтров для мультиплексорных каналов, однако, обладают общим недостатком – сравнительно низким уровнем пропускания. Введение в конструкцию отражающих наноразмерных одномодовых резонаторов приводит к повышению пропускания на их резонансной частоте. Однако для традиционных демультиплексоров, работающих на нескольких частотах, требуется введение нескольких различных резонаторов. В настоящей работе предложена конфигурация трёхканального демультиплексора, использующего один единственный резонатор, причём повышение пропускания для каждого из каналов достигается настройкой резонатора для его работы в многомодовом режиме. Теоретический анализ и компьютерное моделирование показали реализуемость этого подхода, приводящее к двукратному увеличению пропускания для каждого из трёх каналов.

Ключевые слова: *поверхностные плазмоны, фильтрация длины волны, мультиплексирование, субволновая длина.*

INTRODUCTION

With the increasing demand for device response speed, energy consumption and integration degree, traditional electronic devices are becoming more and more difficult to meet people's requirement. Thus, photonic devices with faster response rate, larger bandwidth and higher information efficiency have attracted more and more attention. A hot topic of current research is to realize the effective manipulation of photons at nanometer or subwavelength scale. The common and widely considered waveguide structure has the potential to realize the integration and miniaturization of photonic devices, including: photonic crystal waveguide [1], silicon photonic waveguide [2] and surface plasmon waveguides [3] and related devices, *etc*. Among them, the surface plasmon polaritons (SPPs) based on the metal-dielectric interface can overcome the classical diffraction limit, and realize subwavelength scale manipulation [4–6], catching people's much attention. A variety of surface plasmons based devices such as all-optical switches [7, 8], modulators [9], Mach–Zehnder interferometers [5, 10], beam manipulator [11, 12], polarization analyzer [13], sensors [14, 15], optical amplifier [16], optical buffers [17], Bragg reflectors [18, 19], mirrors [20] and waveguides [21] have been numerically simulated and experimentally demonstrated. With the fast development of technology of nanostructured manufacturing, these devices can be fabricated and applied into high-performance photonic devices in the future.

Because of the short propagation distance of the SPP wave in metal or dielectric, it is constrained in a very small range at the longitudinal direction, while relative acceptable propagation length at the metal dielectric interface make it possible for the use in ultra-small equipment [22]. As a kind of nanoplasmonic wavelength demultiplexer SPP filters based on different kinds of cavities have been put forward and studied [23, 24], however, the transmission efficiency of the channels are relatively low due to the weak resonance effect. For the enhancement of transmission efficiency, reflection cavities are designed by Lu H. *et.al.*, the efficiency has been increased by more than 50%. For a certain cavity, not only fundamental mode but also high order modes can exist. However, when controlling the transmission efficiency of each channel, all of the corresponding reflection cavities need to be tuned due to only fundamental modes were used before. In fact, each mode can be used to enhance the transmission efficiency of channel drop filter. When taking advantage of the multiple modes, isn't it means one cavity can control multi-channel drop filters, simultaneously?

In this paper a new kind of nanoplasmonic wavelength demultiplexing (WDM) structure based on multichannel drop filters in metal-insulator-metal (MIM) waveguide with a single reflection nanocavity is proposed and numerically investigated. The reflection cavity is proposed to control three channels simultaneously. The finite-difference time-domain (FDTD) is used for achieving the simulation results, and temporal coupled-mode theory [25, 26] is used for theoretical analysis. The properties of different modes of resonance in the reflection cavity, and the enhancement of transmission efficiency of the drop waveguide under each mode are discussed.

SIMULATION RESULTS AND ANALYZES

For a certain cavity, different order of modes can exist and decided by cavity parameters. As changing the parameters, resonance frequencies of the modes are changed. Even though the resonance properties of each mode are different in the reflection cavity, these can form coupling mode with that from other cavities so long as their frequencies and the phases can be matched with each other. This means that in the reflection cavity enhanced multichannel drop filter, the coupling between reflection cavity and slot cavity just depends on the same frequencies and the matched phases. Based on this, a MIM structure demultiplexer filter with one reflection cavity for enhancing the transmission efficiency of three channels is designed here.

A cavity with multi modes is discussed at first. Fig. 1a shows the MIM structure schematic of a reflection cavity at one side of the bus waveguide. The width of the bus waveguide slot is fixed to be $w_0 = 50$ nm, the distance between the bus waveguide and the reflection cavity is fixed to be $d_0 = 20$ nm, a and b are the length of the two side of the cavity as Fig. 1a shows. The insulators in the slit and cavity are set as air ($n_d = 1$). The metal is set as Ag, and its frequency dependent relative permittivity is characterized by the well-known Drude model [27]

$$\varepsilon_m(\omega) = \varepsilon_\infty - \frac{\omega_p^2}{\omega(\omega + i\gamma)}, \tag{1}$$

where ε_∞ is the dielectric constant at the infinite frequency, γ and ω_p are the electron collision frequency and bulk plasma frequency, respectively. ω is the angular frequency of incident light. The parameters for Ag is set as ε_∞ =3.7, ω_p = 9.1 eV, and γ = 0.018 eV. TM-polarized plane wave is emitted at P_0. Since the width of the bus waveguide slot is so small, only the fundamental TM mode can be excited in the structure. The dispersion relation is governed by following equations [28]

$$\varepsilon_d k_m + \varepsilon_m k_d \tanh\left(\frac{k_d}{2} w_0\right) = 0, \tag{2}$$

$$k_d = \sqrt{\beta^2 - \varepsilon_d k_0^2}, \quad k_m = \sqrt{\beta^2 - \varepsilon_m k_0^2}, \tag{3}$$

$$n_{\text{eff}} = \beta / k_0, \tag{4}$$

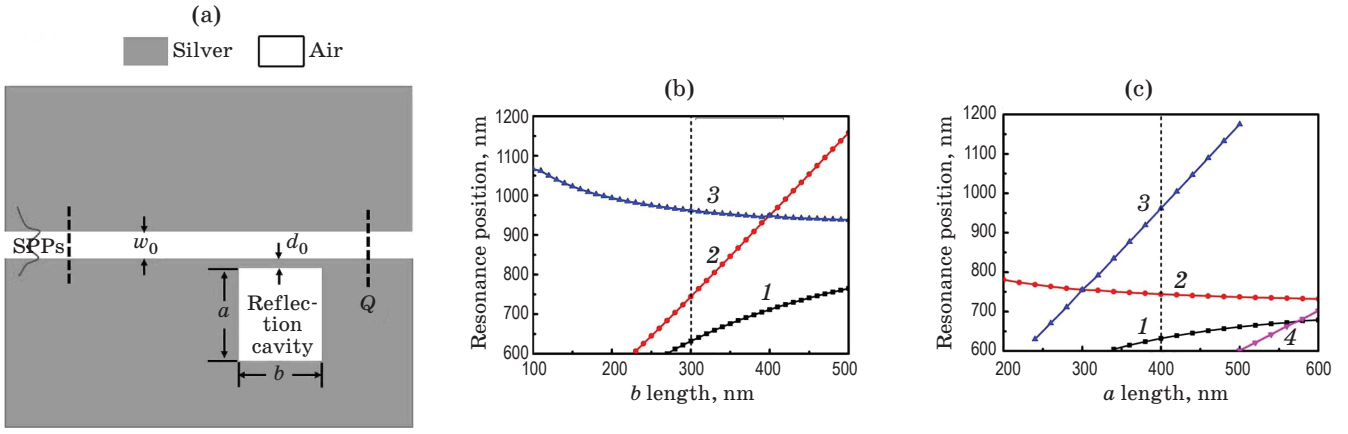

Fig. 1. The schematic of the waveguide with a cavity and its resonance positions at different size. (a) The schematic of the waveguide with a cavity. (b) The resonance positions for the reflection cavity of *b* length dependent resonance modes: *1* — mode 1, *2* — mode 2 and *3* — mode 3. (c) The resonance positions of *a* length dependent resonance modes: *1* — mode 1, *2* — mode 2, *3* — mode 3 and *4* — mode 4.

where ε_m and ε_d are the dielectric constants of the metal and insulator, separately. And $k_0 = \lambda_0/2\pi$ is the free-space wave vector, n_{eff} is the effective dielectric constant, and β is the propagation constant of the SPPs in the MIM structure. The metal is silver and frequency dependent relative permittivity is described with equation (1). In the simulation the spatial grid sizes are set to be 5×5 nm. The incident power is monitored at position *P*, and the transmitted power is monitored at position *Q*. The bus channel transmission efficiency is defined as $T_d = P_P/P_Q$ [29].

When changing the parameters of *a* and *b*, the resonance wavelength modes are changed. Fig. 1b shows the plot of the resonance position different modes evolved with *b* length changed from 100 to 500 nm and a fixed a length of 400 nm. Three curves of modes are shown in Fig. 1b, according to the order of wavelength form shorter to longer they are called mode 1, mode 2 and mode 3, respectively. The wavelength of mode 2 increases similar linearly when *b* increases from 100 to 500 nm. Fig. 1c shows the resonance position changes with a length changes from 200 to 600 nm, when the length of *a* is set to be 300 nm, and four modes shown in Fig. 1c. The mode 3 increases similar linearly when *a* increases from 200 to 600 nm. We choose $a = 400$ nm and $b = 300$ nm as an example as the dash lines shown in Fig. 1b and 1c. Fig. 2a shows three bandstop wavelengths at the chosen parameters. The three bandstop wavelengths are three modes of the cavity. Corresponding incident light wavelengths are 632, 744 and 962 nm, respectively. The electromagnetic distribution localization of mode 1 is along the corners of the cavity, mode 2 is along *a* sides and for mode 3 is along *b* sides [30]. $|H_z|$ distributions of the modes are shown in Fig. 2b, 2c and 2d, separately. We predict that even though the modes are different, reflection wave can obtain to enhance the transmission efficiency of the channel drop filters at certain wavelength, when choosing suitable distance between the drop channels and the reflection cavity.

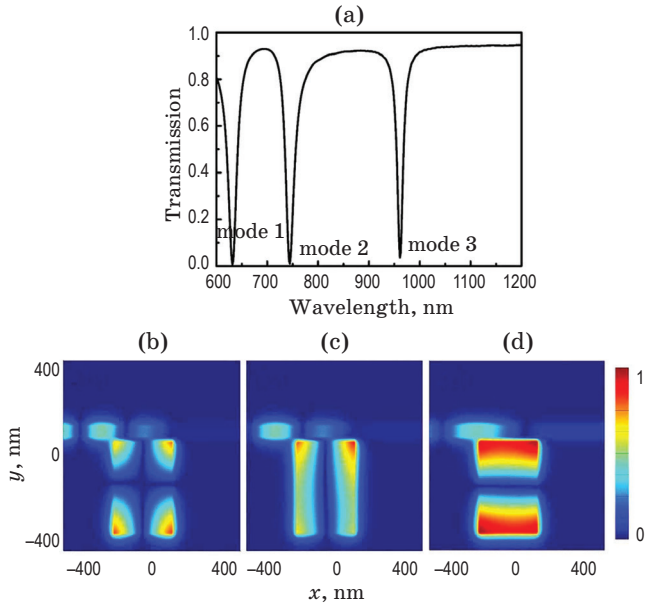

Fig. 2. The transmission efficiency spectra and the $|H_z|$ distribution at each mode. (a) The transmission efficiency at position *Q* when $a = 400$ nm and $b = 300$ nm. The $|H_z|$ distribution at the incident light wavelength of 632 nm (b), 744 nm (c), and $|H_z|$ 962 nm (d).

To get optimal enhanced transmission efficiency, the SPP propagating properties in drop channel need to be analyzed. The existence of the slot cavity, result in SPPs propagating along the bus waveguide slot can be coupled into it and then tunneled into the drop waveguides [31]. The SPPs propagating phase delay per round trip in the slot cavity can be described as $\Delta\varphi = 4\pi n_{\text{eff}} l/\lambda + (\varphi_1 + \varphi_2)$, where φ_1 and φ_2 are the additional phase shifts for the reflection at two sides

of the reflector in the slot cavity, and l is the length of the slot cavity. When the resonance condition of the slot cavity $\Delta\varphi = 2q\pi$ (q is positive integer) is satisfied, the SPPs power can be transmitted into the drop channel. So the transmission wavelengths in the drop channel equal to the resonance wavelength of the slot cavity can be described as

$$\lambda_q = \frac{2n_{\text{eff}}l}{q-(\varphi_1+\varphi_2)/2\pi}. \quad (5)$$

A linear relationship can be seen in Eq. (5), ignores the changing behavior of n_{eff}. According to Eq. (2), we can obtain wavelength dependent effective index n_{eff}. Fig. 3a shows the cavity of the drop channel filter structure, the width of the channel and the cavity slots are also set to be $w_0 = 50$ nm, the distance between cavity slot and bus waveguide slot, and between cavity slot and drop channel slot are both fixed to be $w_t = 15$ nm. The incident power is monitored at position P, and the transmitted power of the drop channel is monitored at position T as shown in Fig. 3a. The drop channel transmission efficiency is defined as $T_d = P_P/P_T$ [29].

Since the reflection cavity is determined, the same resonance wavelength for the slot cavity is required for the enhancement of drop channel transmission efficiency. Fig. 3b shows the cavity length dependent drop channel transmission peak curve. It shows a very good linear relationship, and the fitting curve equation is $\lambda = 180.6 + 2.67l$. Since the reflection cavity shows three oscillation wavelength 632, 744 and 962 nm, corresponding cavity lengths at the same drop channel transmission peak wavelength are calculated, $l_1 = 169$ nm, $l_2 = 211$ nm, and $l_3 = 294$ nm, respectively. Corresponding drop channel transmission efficiency without reflection cavity is only 40, 38 and 33%, and the transmission efficiency spectra are shown in Fig. 3d.

Since the l are decided, the distance between the center of reflection cavity and the slot cavity needs to be decided to obtain maximum enhancement of transmission efficiency, the distance is changed from 0 to 400 nm, the Di (the distance between drop channels and the reflection cavity as shown in Fig. 4a) dependent transmission efficiency of three channels are shown in Fig. 4b, 4c, and 4d, the transmission efficiency period d for the channels are $d_1 = 235$ nm, $d_2 = 260$ nm and $d_3 = 370$ nm, separately. These results can be explained by the temporal coupled-mode theory [25]. As for SPPs wave in metal the wavelength is $\lambda_m = \lambda/n_{\text{eff}}$ which means that the coupling period of reflection cavity and slot cavity $\Delta Di = d = \lambda_m/2 = \lambda/2n_{\text{eff}}$. n_{eff} is the effective refractive index of the SPP mode.

Figures 4b, 4c and 4d show transmission evolution of the channel drop filter with Di from 0 to 400 nm for $l_1 = 169$ nm, $l_2 = 211$ nm and $l_3 = 294$ nm.

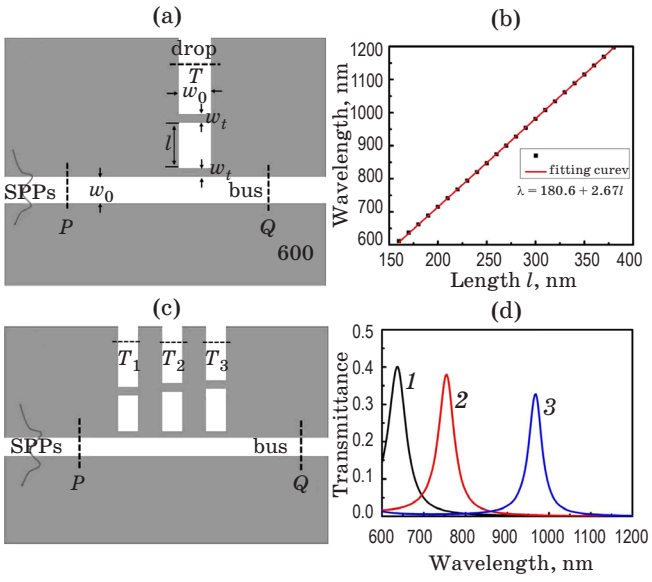

Fig. 3. The schematic of channel drop filter structure based on plasmonic slot cavity and the wavelength change of modes with different slot cavity length. (a) The schematic of channel drop filter structure based on plasmonic slot cavity. (b) The filter wavelength changes with slot cavity length. (c) The schematic of three channels at the filter wavelengths of 632, 744 and 962 nm, separately. (d) The transmission efficiency spectra of three channel drop filters at the slot cavity length of 169 nm (*1*), 211 nm (*2*), and 294 nm (*3*), separately.

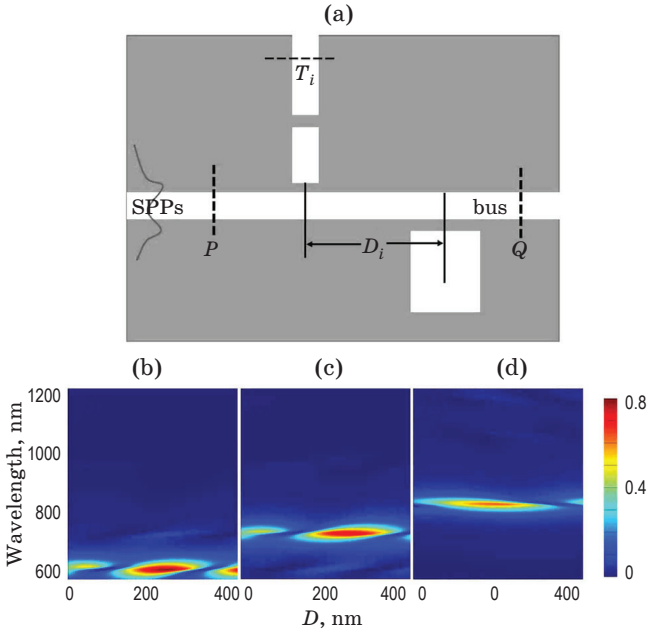

Fig. 4. The schematic of channel drop filter structure with plasmonic slot cavity and reflection cavity and the transmission efficiency spectra with different distence between slot cavity and reflection cavity. (a) The schematic of channel drop filter structure based on plasmonic slot cavity and reflection cavity. Transmission evolution of the channel drop filter with D from 0 to 400 nm for $l_1 = 169$ nm (b), $l_2 = 211$ nm (c), and $l_3 = 294$ nm (d).

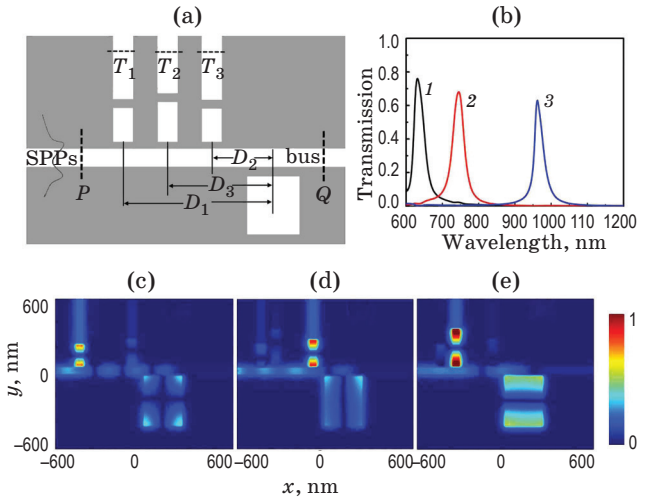

Fig. 5. The schematic of three channel drop filters structure based on plasmonic slot cavity and reflection cavity and optimized transmission efficiency and the $|H_z|$ distribution. (a) The schematic of three channel drop filters structure based on plasmonic slot cavity and reflection cavity. (b) Reflection cavity enhanced transmission efficiency of three channel drop filters at the slot cavity length of 169 nm (*1*), 211 nm (*2*), and 294 nm (*3*), separately. The reflection cavity enhanced the $|H_z|$ distribution at the incident wavelength of 632 nm (c), 744 nm (d), and 962 nm (e).

And also it can be find that the maximum enhancement of transmission efficiency appears when $D_1 = nd_1$, $D_2 = nd_2$ and $D_3 = (n + 1/2)d_3$ (n is positive integer). Which means for $l = 294$ nm the maximum enhancement of transmission efficiency appears when $D = (n - 1/2)d$ (n is positive integer). This difference can be explained by the difference of the resonance properties. The field distributions of $|Hz|$ at each incident light wavelength of the bandstop wavelength are shown in Fig. 2c, 2d, and 2e, respectively.

Considering the periodicity enhancement relation and the non-influence principle of each channel, three slot cavities and drop channels are designed on the other side of the bus waveguide and the distances between slot cavities and reflection cavity are $D_1 = 710$ nm, $D_2 = 250$ nm and $D_3 = 550$ nm for obtaining the maximum enhancement of transmission efficiencies and the schematic of three channel drop filters structure based on plasmonic slot cavity and reflection cavity is shown in Fig. 5a. Simulation results of the enhanced transmission efficiency spectra are shown in Fig. 5b, the transmission efficiencies are 77, 70 and 63%, separately, almost two times stronger than no reflection cavity. The whole structure is less than 1.5 μm of the size but can deal with three different wave bands, simultaneously. And the field distribution of $|H_z|$ are shown in Fig. 5c, 5d and 5e, at the emitted wavelength of 632, 744, and 962 nm, separately.

CONCLUSIONS

In this paper, we designed and studied a new WDM structure, which include a reflection cavity and three drop channel filters. The MIM plasmonic nanostructure is simulated by FDTD, the results indicate that the transmission efficiency of the drop channel filters can be enhanced by a reflection cavity. Even though the resonance modes in the reflection cavity are different, the optimal enhancement of transmission efficiency results is the same. Optimal results show about two times stronger than that without reflection cavity [24]. As an ultracompact structure, this device can be very potential of application in high efficiency WDM systems of highly integrated optical circuits and optical communications.

Funding. National Key Research and Development Program of China (Grant No 2017YFA0207101), National Natural Science Foundation of China (Grant No. 51531006, 11574313, 11374300, and 51571188), Natural Science Foundation of Anhui Province (Grant No. 1508085MA16), and CAS/SAF International Partnership Program for Creative Research Teams.

REFERENCES

1. *Noda S., Fujita M., Asano T.* Spontaneous-emission control by photonic crystals and nanocavities // Nat. Photonics. 2007. № 1. P. 449–458.
2. *Yamada K., Fukuda H., Tsuchizawa T., Watanabe T., Shoji T., Itabashi S.* All-optical efficient wavelength conversion using silicon photonic wire waveguide // Ieee. Photonic. Tech. L. 2006. V. 18. P. 1046–1048.
3. *Liu L., Han Z.H., He S.L.* Novel surface plasmon waveguide for high integration // Opt. Express. 2005. V. 13. P. 6645–6650.
4. *Barnes W.L., Dereux A., Ebbesen T.W.* Surface plasmon subwavelength optics // Nature. 2003. V. 424. P. 824–830.
5. *Bozhevolnyi S.I., Volkov V.S., Devaux E., Laluet J.Y., Ebbesen T.W.* Channel plasmon subwavelength waveguide components including interferometers and ring resonators // Nature. 2006. V. 440. P. 508–511.
6. *Gramotnev D.K., Bozhevolnyi S.I.* Plasmonics beyond the diffraction limit // Nat. Photonics. 2010. V. 4. P. 83–91.
7. Wurtz G.A., Pollard R., Zayats A.V. Optical bistability in nonlinear surface-plasmon polaritonic crystals // Phys. Rev. Lett. 2006. V. 97. P. 057402.
8. *Lu H., Liu X.M., Wang L.R., Gong Y.K., Mao D.* Ultrafast all-optical switching in nanoplasmonic waveguide with Kerr nonlinear resonator // Opt. Express. 2011. V. 19. P. 2910–2915.

9. *Nikolajsen T., Leosson K., Bozhevolnyi S.I.* Surface plasmon polariton based modulators and switches operating at telecom wavelengths // Appl. Phys. Lett. 2004. V. 85. P. 5833–5835.

10. *Wang B., Wang G.P.* Surface plasmon polariton propagation in nanoscale metal gap waveguides // Opt. Lett. 2004. V. 29. P. 1992–1994.

11. *Min C., Wang P., Jiao X., Deng Y., Ming H.* Beam focusing by metallic nano-slit array containing nonlinear material // Appl. Phys. B-Lasers O. 2008. V. 90. P. 97–99.

12. *Yin L.L., Vlasko-Vlasov V.K., Pearson J., Hiller J.M., Hua J., Welp U., Brown D.E., Kimball C.W.* Subwavelength focusing and guiding of surface plasmons // Nano Lett. 2005. V. 5. P. 1399–1402.

13. *Yang S.Y., Chen W.B., Nelson R.L., Zhan Q.W.* Miniature circular polarization analyzer with spiral plasmonic lens // Opt. Lett. 2009. V. 34. P. 3047–3049.

14. *Enoch S., Quidant R., Badenes G.* Optical sensing based on plasmon coupling in nanoparticle arrays // Opt. Express. 2004. V. 12. P. 3422–3427.

15. *D. van Oosten, Spasenovic M., Kuipers L.* Nanohole chains for directional and localized surface plasmon excitation // Nano Lett. 2010. V. 10. P. 286–290.

16. *De Leon I., Berini P.* Amplification of long-range surface plasmons by a dipolar gain medium // Nat. Photonics. 2010. V. 4. P. 382–387.

17. *Gan Q.Q., Ding Y.J., Bartoli F.J.* Rainbow trapping and releasing at telecommunication wavelengths // Phys. Rev. Lett. 2009. V. 102. P. 056801.

18. *Park J., Kim H., Lee B.* High order plasmonic Bragg reflection in the metal-insulator-metal waveguide Bragg grating // Opt. Express. 2008. V. 16. P. 413–425.

19. *Wang B., Wang G.P.* Plasmon Bragg reflectors and nanocavities on flat metallic surfaces // Appl. Phys. Lett. 2005. V. 87. P. 013107.

20. *Randhawa S., Gonzalez M.U., Renger J., Enoch S., Quidant R.* Design and properties of dielectric surface plasmon Bragg mirrors // Opt. Express. 2010. V. 18. P. 14496–14510.

21. *Krasavin A.V., Zayats A.V.* Silicon-based plasmonic waveguides // Opt Express. 2010. V 18. P. 11791–11799.

22. *Dawson P., Defornel F., Goudonnet J.P.* Imaging of surface-plasmon propagation and edge interaction using a photon scanning tunneling microscope // Phys. Rev. Lett. 1994. V. 72. P. 2927–2930.

23. *Tao J., Huang X.G., Zhu J.H.* A wavelength demultiplexing structure based on metal-dielectric-metal plasmonic nano-capillary resonators // Opt. Express. 2010. V. 18. P. 11111–11116.

24. *Hu F.F., Yi H.X., Zhou Z.P.* Wavelength demultiplexing structure based on arrayed plasmonic slot cavities // Opt. Lett. 2011. V. 36. P. 1500–1502.

25. *Manolatou C., Khan M.J., Fan S.H., Villeneuve P.R., Haus H.A., Joannopoulos J.D.* Coupling of modes analysis of resonant channel add-drop filters // Ieee. J. Quantum Elect. 1999. V. 35. P. 1322–1331.

26. *Lu H., Liu X.M., Gong Y.K., Mao D., Wang L.R.* Enhancement of transmission efficiency of nanoplasmonic wavelength demultiplexer based on channel drop filters and reflection nanocavities // Opt. Express. 2011. V. 19. P. 12885–12890.

27. *Han Z.H., Forsberg E., He S.L.* Surface plasmon Bragg gratings formed in metal-insulator-metal waveguides // Ieee. Photonic Tech. L. 2007. V. 19. P. 91–93.

28. *Dionne J.A., Weathercock L.A., Atwater H.A., Polman A.* Plasmon slot waveguides: Towards chip-scale propagation with subwavelength-scale localization // Physical Review B. 2006. V. 73. P. 035407.

29. *Lin X.S., Huang X.G.* Tooth-shaped plasmonic waveguide filters with nanometeric sizes // Opt. Lett. 2008. V. 33. P. 2874–2876.

30. *Noual A., Akjouj A., Pennec Y., Gillet J.N., Djafari-Rouhani B.* Modeling of two-dimensional nanoscale Y-bent plasmonic waveguides with cavities for demultiplexing of the telecommunication wavelengths // New J. Phys. 2009. V. 11. P. 103020.

31. *Lan Y.C., Chang C.J., Lee P.H.* Resonant tunneling effects on cavity-embedded metal film caused by surface-plasmon excitation // Opt. Lett. 2009. V. 34. P. 25–27.